



Cite this: *Chem. Commun.*, 2016, 52, 11991

Received 27th July 2016,  
Accepted 6th September 2016

DOI: 10.1039/c6cc06203b

www.rsc.org/chemcomm

## Synthesis and deposition of a Tröger's base polymer on the electrode surface for potentiometric detection of a neuroblastoma tumor marker metabolite†

T. V. Shishkanova,<sup>\*a</sup> M. Havlík,<sup>a</sup> M. Dendisová,<sup>b</sup> P. Matějka<sup>b</sup> and V. Král<sup>\*a</sup>

The development of novel diagnostic tools is a primary goal in bioanalytical chemistry. Here we report the synthesis of Tröger's base functionalized with amino- and coumarin-units designed as a monomeric unit for the development of an electrochemical cancer sensor. The synthesized receptor was deposited onto a conducting support using electrochemical polymerization, characterized spectroscopically and tested potentiometrically towards metabolites used as tumor markers of neuroblastoma.

The development of detection methods for diseases with high mortality represents a crucial target of contemporary science. At present, the classical methodology for cancer detection is based on biopolymer analysis.<sup>1–5</sup> A modern innovative approach is based on low-molecular weight non-classical tumor markers (TMs) and cancer cell metabolite identification.<sup>6–8</sup> Despite the potential significance of detection of low-molecular weight non-classical TMs, there have been no reports on their determination using supramolecular analytical chemistry, especially potentiometry.<sup>9</sup> Neuroblastoma, a neuroblastic tumor derived from the primordial neural crest, remains the leading cause of disease in infancy. A promising screening test for neuroblastoma could rely on the monitoring of urine catecholamine metabolites, namely homovanillic acid (HVA) and vanillylmandelic acid (VMA) (Fig. 1), which serve as TMs.<sup>10</sup>

Ultrasensitive diagnostic devices based on electrochemical principles could be quite a simple approach to screening the low-molecular-weight non-classical TMs of neuroblastoma. Recently, Nemiroski *et al.* have proposed universal mobile and highly effective electrochemical devices for the detection of (i) glucose in the blood for personal health, (ii) sodium in urine for clinical analysis, and (iii) a malarial antigen for

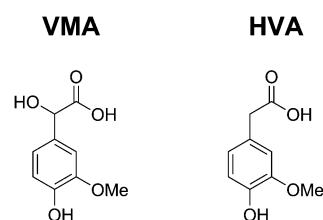


Fig. 1 The structures of the tested metabolites for screening neuroblastoma.

clinical research.<sup>11</sup> The compatibility of similar devices with any mobile phone or wearable electronics guarantees that sophisticated diagnostic testing can be performed by users with a broad spectrum of needs, resources, and levels of technical expertise. A few reports have been related to voltammetric determination of HVA and VMA without using supramolecular receptors.<sup>12</sup>

Since a number of biologically relevant molecules are electro-active, the selectivity of many electrochemical sensors based on electroactivity is limited. Therefore, a promising way to avoid overlapping electrochemical signals and increase selectivity is the development of a potentiometric sensor derived from a recognition receptor selective towards the low-molecular-weight target metabolite. We pioneered potentiometric determination of the metabolites for neuroblastoma screening.

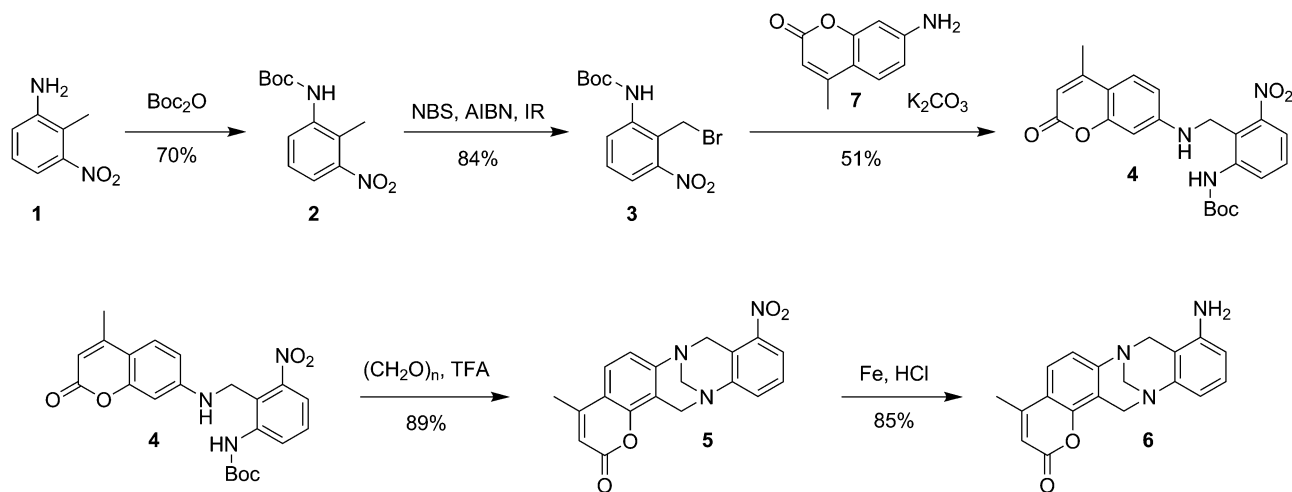
Tröger's base is a molecule containing two arenes connected to the *b* and *f* sides of 1,5-methano-1,5-diazocine.<sup>13,14</sup> Due to its unique structural features ( $C_2$ -symmetry and rigid V-shape geometry) and the possibility of functionalization, Tröger's base is an attractive receptor for the development of optical and spectroscopic sensors.<sup>13–16</sup> The sensor technology assumes immobilization of a supramolecular receptor onto the electrode interface between the transducer and the measured sample. The practically applicable approach is to immobilize a receptor into a suitable matrix. However, a non-covalently immobilized monomer can leach out from the matrix as a result of desorption and other physical effects occurring on the electrode surface in contact with the sample. In contrast, covalent immobilization of

<sup>a</sup> Department of Analytical Chemistry, University of Chemistry and Technology in Prague, 16628 Prague 6, Technická 5, Czech Republic.

E-mail: tatiana.shishkanova@vscht.cz, shishkat@yahoo.com, kralv@vscht.cz

<sup>b</sup> Department of Physical Chemistry, University of Chemistry and Technology in Prague, 16628 Prague 6, Technická 5, Czech Republic

† Electronic supplementary information (ESI) available: Details of synthetic experimental. See DOI: 10.1039/c6cc06203b



**Scheme 1** Stepwise preparation protocol of Tröger's base functionalized with amino- and coumarin-units **6**.

a receptor allows limiting the leaching out from the sensor surface and constructing microsensors for practical applications. In this communication, a Tröger's base derivative **6** (Scheme 1) was designed to allow us to deposit it electrochemically on the electrode surface and to detect the metabolite in question potentiometrically. The success of the supramolecular design was proven using spectroscopic and nanoscopic experiments, comprising both optical and mechanical measurements. Scheme 1 shows the synthesis of receptor **6**.†

We should note that this is not a case of preparation of a molecularly imprinted polymer. TMs are not present in the electropolymerization mixture.† A cyclic voltammogram of **6** on a Pt electrode (Fig. 2) exhibits two anodic peaks at *ca.* 0.55 and 1.02 V (from the 1st potential scan) and the reduction peak at *ca.* 0.47 V. The current intensity increased from 1 to 4 cycles, indicating the polymer growth (Fig. 2). In the subsequent scans, the current decreased, indicating the growth of the non-conducting polymeric film. The presence of the anodic peak at 1.02 V is related to the oxidation of the monomer and

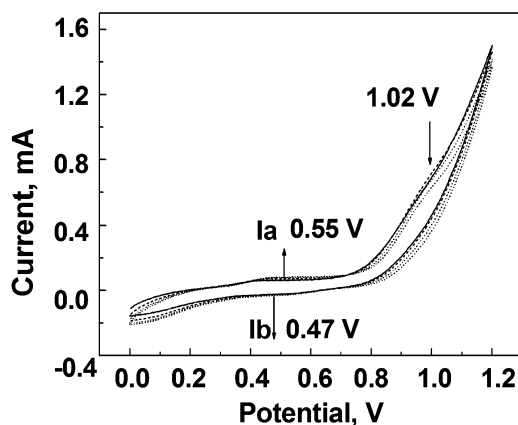


**Fig. 2** Cyclic voltammogram of a Tröger's base derivative **6** in  $\text{CH}_3\text{CN}$ /TBAFB/HCl on a Pt electrode. The electrode potential was swept repeatedly between 0.0 and 1.2 V vs. Ag/AgCl at a scan rate of  $50 \text{ mV s}^{-1}$ ; the number of scans is 4.†

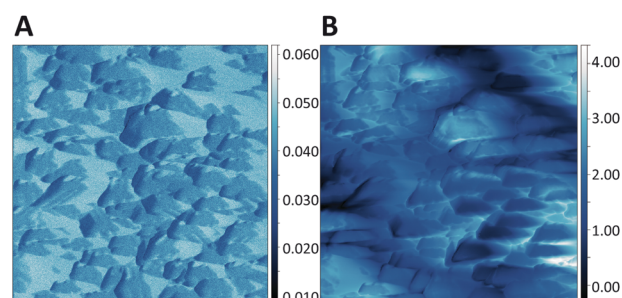


**Fig. 3** SNIM images:  $5 \times 5 \mu\text{m}$  of the Au electrode surface. Mechanical amplitude signal (A) and optical signal (B).

initiation of the electrosynthesis of the polymeric film.<sup>17</sup> A couple (peaks **Ia** and **Ib**) is evident at a potential of *ca.* 0.55 V, corresponding to the reduction-oxidation of an adsorbed product.

Scanning near-field infrared microscopy (SNIM) combined with nanomechanical patterning shows that the polymeric film on the electrode surface is nanostructured and consists of "hills" and "valleys" with a maximal height profile of  $0.5 \mu\text{m}$  (Fig. 3A). The amplitude of the infrared signal assigned to the aromatic C–C stretching mode suggests that the adhering film is porous, with grains located on the edges of both "hills" and "valleys" (Fig. 3B).

To confirm the formation of the polymer derived from **6**, Fourier transform infrared (FTIR) spectra of the monomer and the polymer prepared by chemical polymerization in  $\text{CH}_3\text{CN}$  were compared (Fig. 4). The polymer spectrum differs substantially from that of the monomer between  $3400$  and  $3200 \text{ cm}^{-1}$  and under  $1600 \text{ cm}^{-1}$ . In contrast to the monomer spectrum, which exhibits bands at  $\sim 3350 \text{ cm}^{-1}$  and  $\sim 3237 \text{ cm}^{-1}$  assigned to a primary amino group, the polymer spectrum exhibits the band at  $\sim 3217 \text{ cm}^{-1}$  of the secondary amino group.<sup>18</sup> The intensity ratio of bands at *ca.*  $2960 \text{ cm}^{-1}$  and  $2930 \text{ cm}^{-1}$  of asymmetric stretching vibrations of  $\text{CH}_3$  and  $\text{CH}_2$  groups, respectively, is reversed. These changes may be rationalized as follows: in the methylcoumarin unit, the possible delocalization of electrons in the lactone ring taking place during polymerization leads to the change in the

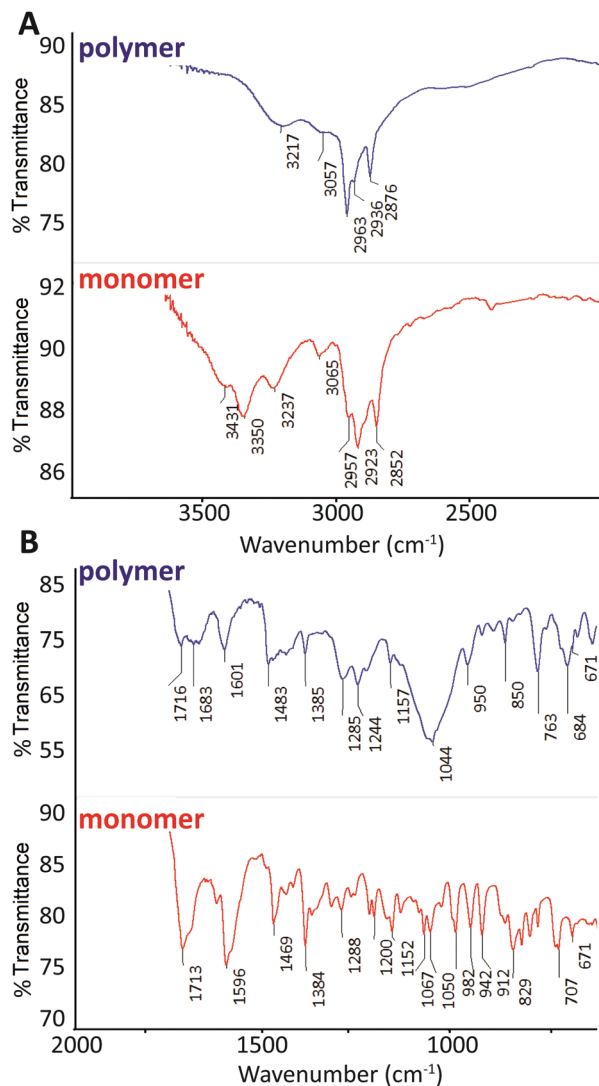


Fig. 4 FTIR spectra of the polymer (blue) and the monomer (red) from 4000 to 2000  $\text{cm}^{-1}$  (A) and from 1900 to 600  $\text{cm}^{-1}$  (B). Each spectrum was averaged from 256 scans with 4  $\text{cm}^{-1}$  resolution.

dipole moment of  $\text{CH}_3$  vibrations and to the conformational changes. The bands at 1713 and 1716  $\text{cm}^{-1}$  of the  $\text{C}=\text{O}$  vibration of the coumarin unit are observed in both the monomer and polymer spectra, respectively. After polymerization, the intensity of the coupled N-H and C-C vibration band at 1683  $\text{cm}^{-1}$  is remarkably increased to a level comparable to the  $\text{C}=\text{O}$  vibration.<sup>19</sup> The aromatic ring modes are shown as a set of bands under 1600  $\text{cm}^{-1}$  (1596, 1469, 1288, 1152, 1067, 1050, 942, 829 and 707  $\text{cm}^{-1}$ ) in both spectra with different intensities. We note that the  $\text{C}=\text{N}$  stretching vibration at 1483  $\text{cm}^{-1}$  assigned to the benzenoid units<sup>20</sup> characteristic of polyaniline is observed in the polymer spectrum. The intense band at 1044  $\text{cm}^{-1}$  results from the sulfate anion as a product of aniline oxidation by persulfate and somewhat overlaps with the band at ca. 1140  $\text{cm}^{-1}$  assigned to protonated polyaniline.<sup>18</sup> Hence the FTIR spectra reveal the polymerization of **6** via its amino group according to the mechanism of aniline polymerization.

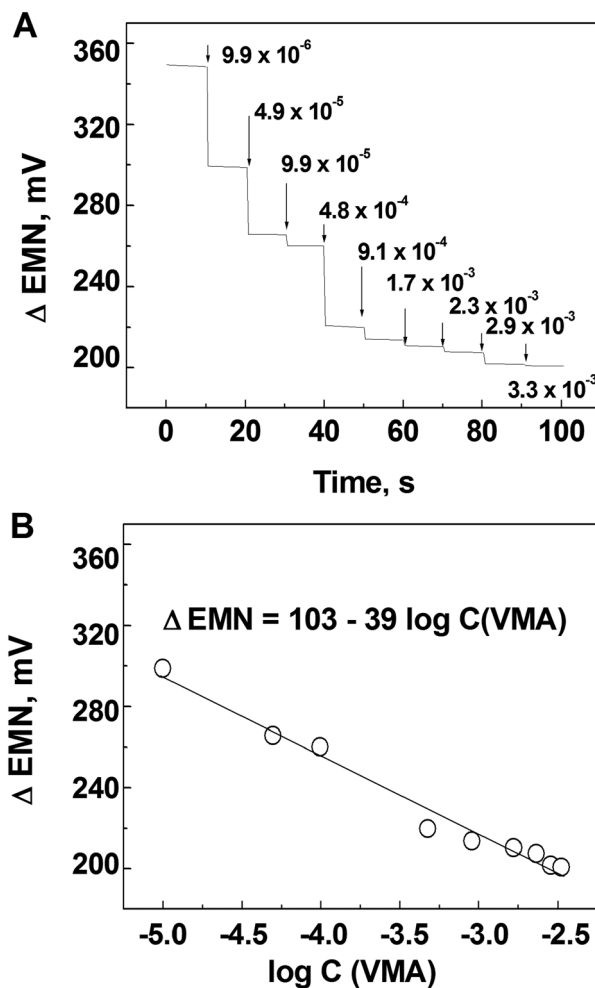


Fig. 5 (A) Potentiometric response and (B) calibration graph of the electrode modified with the polymer based on **6** towards VMA in 0.1  $\text{mol L}^{-1}$  phosphate buffer at pH = 7.

The electrochemically modified electrodes were tested for the potentiometric detection of TMs (Fig. 5).† A potentiometric response of  $-39 \text{ mV decade}^{-1}$  towards VMA was found in the concentration range from  $9.9 \times 10^{-6}$  to  $3.3 \times 10^{-3} \text{ mol L}^{-1}$  (the squared correlation coefficient was equaled 0.9914). The under-Nernstian behavior could be caused by the roughness of the polymeric film and the effect of the surface morphology of the supporting metallic material. In the case of HVA, the potentiometric response of the prepared electrode was insignificant (not shown). The tested TMs are structurally closely related (Fig. 1) and differ by the hydroxy group present in VMA. The potentiometric findings indicate that the electrode based on the polymer derived from **6** enables the selective detection of VMA in the presence of HVA ( $\log K_{\text{VMA, HVA}}^{\text{Pot}} = -0.9$ ).† That a polymer film prepared from Tröger's base prefers VMA to HVA may be a result of both its spatial arrangement and accessibility of binding sites for tested TMs into the polymeric film on the electrode surface. Actually, our spectroscopic findings confirmed that the conformational changes take place during electropolymerization. The hydroxyl groups of VMA (Fig. 1) may reinforce

hydrogen bonding between VMA and the polymeric film.<sup>21</sup> For infants (0–1 year old) and children (1–13 years old), the level of the analyzed TMs is  $(1.0\text{--}5.4) \times 10^{-5} \text{ mol L}^{-1}$  in urine.<sup>22</sup> The content of TMs exceeding the above-mentioned range 10 times is a signal of concern.<sup>23</sup> Experiments were conducted to measure the concentration of VMA added to an artificial urine.<sup>24</sup> It was found to be  $(6 \pm 2) \times 10^{-5} \text{ mol L}^{-1}$  ( $n = 3$ ) VMA when  $5 \times 10^{-5} \text{ mol L}^{-1}$  VMA was introduced. These results indicated that the constituents of the prepared urine sample do not interfere with the VMA detection and the proposed electrode based on the Troger's base polymer provides an alternative device for VMA determination.

In conclusion, we have presented an innovative detection of a neuroblastoma TM which is based on specific and selective interaction with a polymer film (prepared from **6**) and VMA. The detection was purely potentiometric. The geometry of electrochemically polymerized receptor **6** enabled it to interact specifically with VMA in contrast to HVA.

This work was supported by the Grant Agency of the Czech Republic (Project P206/15/02815S), Grant No. LH14008 (Kontakt II) and by the Technology Agency of the Czech Republic, Grant No. TE01020028.

## Notes and references

- 1 S. Ge, L. Ge, M. Yan, X. Song, J. Yu and J. Huang, *Chem. Commun.*, 2012, **48**, 9397.
- 2 S. K. Basak and E. S. Srivatsan, in *Cancer Biomarker: minimal and noninvasive early diagnosis and prognosis*, Salivary biomarkers in early diagnosis of cancer. D. Barh, A. Carpi, M. Verma and M. Gunduz, CRC Press-Taylor & Francis group, 6000 Broken Sound Parkway NW, STE 300, Boca Raton, FL 33487-2742 USA, 2014, pp. 159–195.
- 3 G. K. Joshi, S. Deitz-McElyea, T. Liyanage, K. Lawrence, S. Mali, R. Sardar and M. Korc, *ACS Nano*, 2015, **9**, 11075.
- 4 P. E. Swanson, *Appl. Immunohistochem. Mol. Morphol.*, 2015, **23**, 81.
- 5 S. Srivastava, B. J. Reid, S. Ghosh and B. S. Kramer, *J. Cell. Physiol.*, 2016, **231**, 1870.
- 6 Y. Lu, N. Li, L. Gao, Y.-J. Xu, C. Huang, K. Yu, Q. Ling, Q. Cheng, S. Chen, M. Zhu, J. Fang, M. Chen and C. N. Ong, *Cancer Res.*, 2016, **76**, 2912.
- 7 K. Kim, S.-G. Yeo and B. C. Yoo, *Cancer Res. Treat.*, 2015, **47**, 78.
- 8 B. Muthuraj, S. Mukherjee, S. R. Chowdhury, C. R. Patra and P. K. Iyer, *Biosens. Bioelectron.*, 2015, DOI: 10.1016/j.bios.2015.12.036.
- 9 (a) J. Wang, *Biosens. Bioelectron.*, 2006, **21**, 1887; (b) B. Bohunicky and S. A. Mousa, *Nanotechnol., Sci. Appl.*, 2011, **4**, 1.
- 10 T. Manickum, *J. Chromatogr. B: Anal. Technol. Biomed. Life Sci.*, 2009, **877**, 4140.
- 11 A. Nemiroski, D. C. Christodouleas, J. W. Hennek, A. A. Kumar, E. J. Maxwell and M. T. Fernandez-Abedul, *Proc. Natl. Acad. Sci. U. S. A.*, 2014, **111**, 11984.
- 12 (a) M. C. Blanco-Lopez, M. J. Lobo-Castanon, A. J. Miranda-Ordieres and P. Tunon-Blanco, *Biosens. Bioelectron.*, 2003, **18**, 353; (b) Q. Li, C. Batchelor-McAuley and R. G. Compton, *J. Phys. Chem.*, 2010, **114**, 9713.
- 13 B. Dolensky, J. Elguero, V. Kral, C. Pardo and M. Valik, *Adv. Heterocycl. Chem.*, 2007, **93**, 1.
- 14 S. Sergeyev, *Helv. Chim. Acta*, 2009, **92**, 415.
- 15 B. Baldeyrou, C. Tardy, C. Bailly, P. Colson, C. Houssier, F. Charmantray and M. Demeunynck, *Eur. J. Med. Chem.*, 2002, **37**, 315.
- 16 R. B. P. Elmes, M. Erby, S. A. Bright, D. C. Williams and T. Gunnlaugsson, *Chem. Commun.*, 2012, **48**, 2588.
- 17 H. Lund and M. M. Baizer, *Organic Electrochemistry*, Marcel Dekker, New York, NY, 1991.
- 18 M. Trchová, Z. Morávková, I. Šeděnková and J. Stejskal, *Chem. Pap.*, 2012, **66**, 415.
- 19 E. Kavitha, N. Sundaraganesan and S. Sebastian, *Indian J. Pure Appl. Phys.*, 2010, **48**, 20.
- 20 S. A. Hassoon, *Int. J. Innovative Res. Sci., Eng. Technol.*, 2014, **3**, 9763.
- 21 Y. Diñeiro, M. I. Menéndez, M. C. Blanco-López, M. J. Lobo-Castañón, A. J. Miranda-Ordieres and P. Tuñón-Blanco, *Anal. Chem.*, 2005, **77**, 6741.
- 22 D. S. Wishart, R. Mandal, A. Stanislaus and M. Ramirez-Gaona, *Metabolites*, 2016, **6**, 10.
- 23 S. C. Gates, C. C. Sweeley, W. Krivit, D. DeWitt and B. E. Blaisdell, *Clin. Chem.*, 1978, **24**, 1680.
- 24 N. Laube, B. Mohr and A. Hesse, *J. Cryst. Growth*, 2001, **233**, 367.

